B cell-intrinsic TLR7 signaling is required for neutralizing antibody responses to SARS-CoV-2 and pathogen-like COVID-19 vaccines

Charles-Henry Miquel, Flora Abbas, Claire Cénac, Charlotte Foret-Lucas, Chang Guo, Mariette Ducatez, Etienne Joly, Baidong Hou, Jean-Charles Guéry

European Journal of Immunology Clinical·Basic·Translational

Immunity to infection

Clinical

Short Communication

B cell-intrinsic TLR7 signaling is required for neutralizing antibody responses to SARS-CoV-2 and pathogen-like COVID-19 vaccines

Charles-Henry Miquel[1,2], Flora Abbas[1], Claire Cenac[1], Charlotte Foret-Lucas[3], Chang Guo[4,5], Mariette Ducatez[3], Etienne Joly[6], Baidong Hou[4,5] and Jean-Charles Guéry[1]

[1] Institut Toulousain des Maladies Infectieuses et Inflammatoires (INFINITY), Université de Toulouse, INSERM, CNRS, UPS, Toulouse, France
[2] Arthritis R&D, Neuilly-Sur-Seine, France
[3] Interactions Hôtes Agents Pathogènes (IHAP), UMR1225, Université de Toulouse, INRAe, ENVT, Toulouse, France
[4] CAS Key Laboratory of Infection and Immunity, CAS Center for Excellence in Biomacromolecules, Institute of Biophysics, Chinese Academy of Sciences, Beijing, China
[5] College of life Science, University of Chinese Academy of Sciences, Beijing, China
[6] Institute of Pharmacology and Structural Biology (IPBS), University of Toulouse, CNRS, Toulouse, France

Toll-like receptor 7 (TLR7) triggers antiviral immune responses through its capacity to recognize single-stranded RNA. *TLR7* loss-of-function mutants are associated with life-threatening pneumonia in severe COVID-19 patients. Whereas TLR7-driven innate induction of type I IFN appears central to control SARS-CoV2 virus spreading during the first days of infection, the impact of *TLR7*-deficiency on adaptive B-cell immunity is less clear. In the present study, we examined the role of TLR7 in the adaptive B cells response to various pathogen-like antigens (PLAs). We used inactivated SARS-CoV2 and a PLA-based COVID-19 vaccine candidate designed to mimic SARS-CoV2 with encapsulated bacterial ssRNA as TLR7 ligands and conjugated with the RBD of the SARS-CoV2 Spike protein. Upon repeated immunization with inactivated SARS-CoV2 or PLA COVID-19 vaccine, we show that *Tlr7*-deficiency abolished the germinal center (GC)-dependent production of RBD-specific class-switched IgG2b and IgG2c, and neutralizing antibodies to SARS-CoV2. We also provide evidence for a non-redundant role for B-cell-intrinsic TLR7 in the promotion of RBD-specific IgG2b/IgG2c and memory B cells. Together, these data demonstrate that the GC reaction and class-switch recombination to the Myd88-dependent IgG2b/IgG2c in response to SARS-CoV2 or PLAs is strictly dependent on cell-intrinsic activation of TLR7 in B cells.

Keywords: Adaptive B-cell immunity · Germinal center · RBD · SARS-CoV2 · TLR7

Additional supporting information may be found online in the Supporting Information section at the end of the article.

Correspondence: Dr. Jean-Charles Guéry
e-mail: jean-charles.guery@inserm.fr

Introduction

Toll-like receptor 7 (TLR7) is essential for the induction of antiviral immunity through its capacity to elicit strong type I IFN production in plasmacytoid dendritic cells (pDCs) and to

promote B-cell activation and germinal center (GC) responses [1, 2]. TLR7 is a receptor for single-stranded RNA, encoded by an X-linked gene, maintained under strong purifying selection, which attests to its non-redundant biological role in host survival [3]. In multiple studies, however, rare *TLR7* genetic variants suppressing or modifying the function of the receptor have been identified in young male patients affected by severe COVID-19 [4–7]. Some of these variants were associated with impaired type I IFN response upon TLR7 stimulation supporting the importance of intact TLR7 signaling in pDCs in the early control of COVID-19 pathogenesis [4, 7]. Indeed, SARS-CoV2 can induce type I IFN production in human and mouse pDCs [8, 9], and *TLR7*-deficiency can abolish pDC activation by intact or inactivated viruses in humans [7] and mice [9], respectively. However, the impact of TLR7-deficiency on the generation of protective humoral immune response upon natural infection with SARS-CoV2 or vaccination with a virus-derived nanoparticle-based COVID-19 vaccine is less clear.

A key role for TLR7 has been established in the GC responses to ssRNA viruses and virus-like particles (VLP) [10]. B-cell-intrinsic Myd88/TLR7 signaling is essential to the GC responses to exogenous retrovirus [11]. In chronic lymphocytic choriomeningitis virus (LCMV) infection, B-cell-intrinsic TLR7 signaling is also required for optimal B-cell responses and GC formation [12, 13]. Bacterial phage Qβ virus-like particles (VLP) have emerged as a useful model to study the TLR-dependent activation and differentiation of Ag-specific B cells under a physiological context in vivo [10, 14]. Qβ-VLP can package host bacterial ssRNA and are therefore equipped with a unique feature of natural pathogens, which can serve as a potent TLR7 ligand to promote Ab production and GC responses [10, 14]. Indeed, it has been established that Myd88-signaling in B cells was critical for the anti-Qβ-VLP GC response [10, 14]. This model likely represents the antiviral response more closely than the T-cell-dependent antibody responses to soluble protein antigens and pointed to a critical non-redundant role of Myd88-driven B-cell activation in GC reaction [10, 14]. Indeed, it has recently been reported by using this model that B cells are the dominant Ag-presenting cells inducing naive CD4 T-cell activation and differentiation in response to vaccination with either Qβ-VLP or influenza virus [15]. Again, B-cell-intrinsic Myd88-signaling was required for this process, further suggesting the critical function of TLR7-activated B cells in the generation of T-cell-dependent GC response to RNA viruses, as opposed to the role of DC in the GC response to soluble protein Ag [15].

In the present study, we directly investigated the requirement for TLR7 expression in the generation of neutralizing antibodies specific for the receptor binding domain (RBD) of SARS-CoV2 upon immunization with pathogen-like antigens (PLA)-based COVID-19 vaccines. PLA-based platforms, such as VLPs that encapsulate TLR ligands have been successfully used to promote efficient immune responses including protective immunity to SARS-CoV2 [16, 17]. As PLAs, we used beta-propiolactone (BPL) inactivated SARS-CoV2, and AP205-RBD VLPs, designed to structurally mimic SARS-CoV2 with encapsulated bacterial ssRNA as TLR7 ligands and conjugated with the RBD of the SARS-CoV2 spike protein [17].

Results and discussion

Quantification of anti-RBD IgG isotypes in serum from BPL-inactivated SARS-CoV2 immunized mice

To monitor RBD-specific antibodies, we adapted the HAT (HemAgglutination test) method based on a single reagent, IH4-RBD, which binds to human RBC via the IH4 nanobody specific for human Glycophorin A, creating a matrix of RBD epitopes on the surface of human RBC [18]. IH4-RBD coated human RBC were then incubated with serum from SARS-CoV2 immunized mice and the bound RBD-specific IgG were then detected using isotype-specific PE-labelled monoclonal antibodies (Fig. S1A). No significant binding was observed in the absence of IH4-RBD coating (Fig. S1B) and when RBC were coated with IH4 alone (Fig. S1C). Results were expressed as geometric mean fluorescence intensity (GMFI) thereby offering a much broader dynamic range of quantification over several logs than a commercial ELISA test, in agreement with other works using FACS-based assay to detect anti-SARS-CoV2 antibody [19–21]. Moreover, the method is highly reproducible (Fig. S1D,E). We used this assay to quantify the primary RBD-specific IgG response between WT and TLR7-deficient mice immunized with BPL-inactivated SARS-CoV2 (Fig. S2). Whereas anti-RBD IgG1 activities were detected with similar magnitude and kinetics in both groups (Fig. S2A,D), TLR7-deficient mice were unable to mount detectable RBD-specific IgG2b and IgG2c (Fig. S2B,C,E,F). The neutralizing Ab titers (NAb) were determined at day 25 (Fig. S2G). At this early time point, NAb were selectively detected in WT but not in TLR7-deficient mice, and were positively correlated with IgG2c RBD-specific activity (Fig. S2G,H). Together, these results show that the HAT-flow assay designed with IH4-RBD coated HuRBC is highly sensitive, reproducible, and offers a dynamic quantification of the RBD-specific IgG isotypes in mice immunized with SARS-CoV2.

TLR7 is required for RBD-specific IgG2b/2c and NAb production upon immunization with BPL-SARS-CoV2

We then tested the impact of TLR7-deficiency on the generation of neutralizing anti-RBD antibodies (NAb) upon secondary and tertiary challenges with BPL-SARS-CoV2. Secondary immunization dramatically boosted the RBD-specific IgG activities in WT mice by about 10-fold (Fig. 1A–C). Again TLR7-deficient mice failed to mount significant secondary IgG2b and IgG2c responses to RBD (Fig. 1B,C), and failed to generate detectable anti-SARS-CoV2 Nabs at all time points post-secondary challenge (Fig. 1D) despite high levels of RBD-specific IgG1 (Fig. 1A). In agreement, with our analysis during the primary response (Fig. S2), NAb titers were positively correlated to RBD-specific IgG2c but not to the other isotypes (Fig. 1E). We then investigated whether repeated

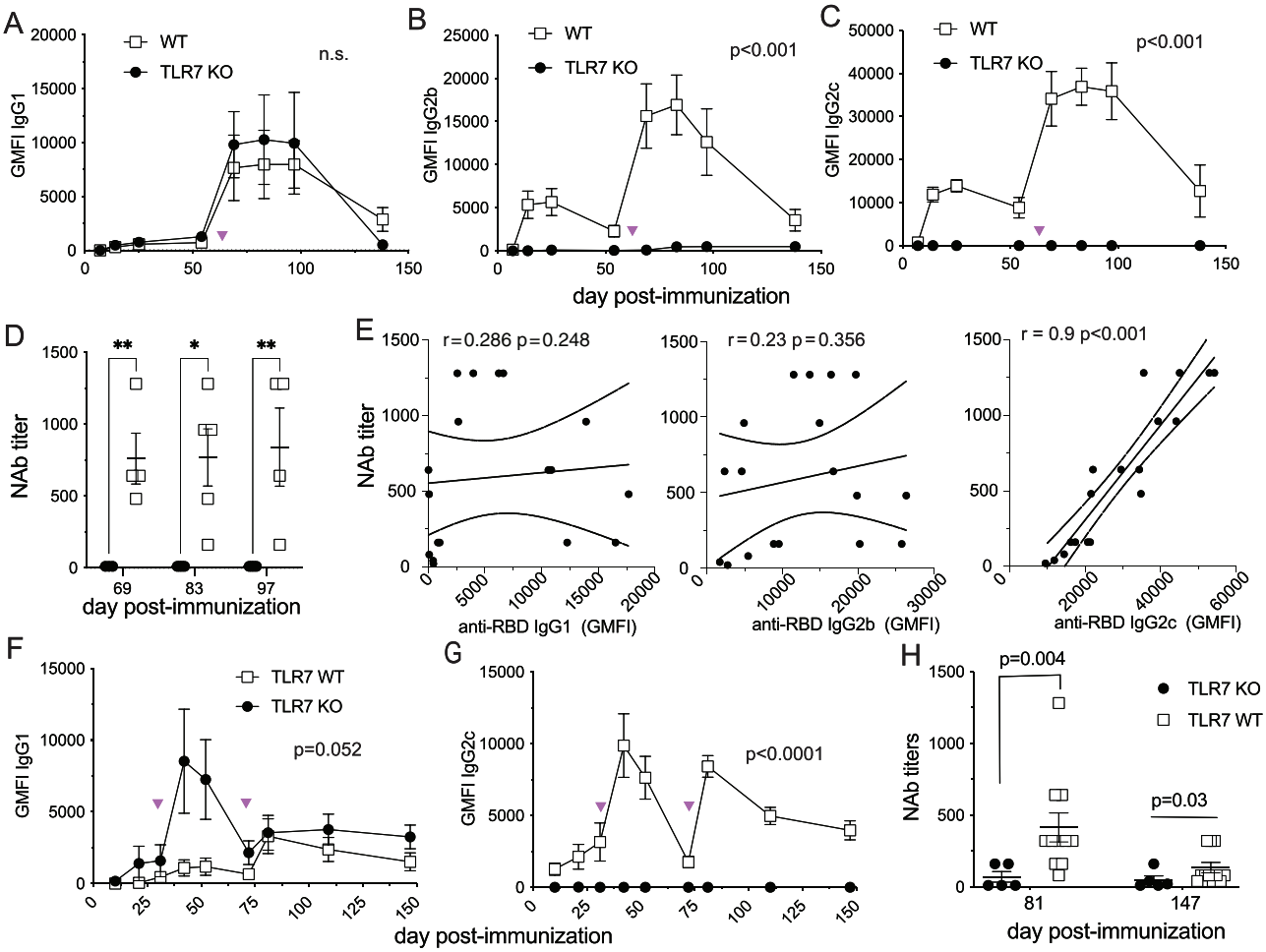

Figure 1. Prime/boost immunization with BPL-inactivated SARS-CoV2 induces high titers of neutralizing IgG2c antibodies in WT but not in TLR7-deficient mice. (A–E) WT and TLR7-deficient B6 female mice were immunized i.p. with BPL-SARS-CoV2 (15μg/mouse) and challenged (7.5 μg/mouse) at day 62. The relative production of RBD-specific IgG isotypes IgG1 (A), IgG2b (B), and IgG2c (C) was quantified in mouse sera at the indicated time points using the HAT-Flow assay as described in Fig. S1. Results are expressed as GMFI with background subtracted from 4–5 mice/group (mean ±SEM). (D) Seroneutralization assay on Vero E6 cells was used to determine the neutralizing Ab titers (NAb). Statistical differences between groups were assessed using the mixed-effects model. (E) The correlation between the NAb titers and the RBD-specific IgG1, IgG2b, or IgG2c activities in bleeding collected between day 54 and 97 was analyzed using the Spearman test. (F, G) WT (n = 6) and TLR7-deficient (n = 5) B6 female mice were immunized i.p. with BPL-SARS-CoV2 (15μg/mouse), and then challenged at day 31 and day 72. The kinetics of the RBD-specific IgG1 and IgG2c antibodies was measured as above. Arrowheads indicate the time points for secondary or tertiary immunization. Statistical differences between groups were analyzed using a two-way-ANOVA test. (H) The neutralizing Ab titers were determined in individual mice at the indicated time points following the tertiary challenge. Results (A–E and F–H) are from two independent experiments. Statistical differences were analyzed using a Mann–Whitney test.

immunization with inactivated SARS-CoV2 could promote RBD-specific NAb in the absence of *Tlr7* gene. Mice were immunized and then boosted at days 31 and 72 with the same dose of inactivated vaccine. In this experiment, we confirmed the complete switch in RBD-specific IgG isotypes between WT and TLR7-deficient mice, which produced preferentially anti-RBD IgG1 antibodies (Fig. 1F), but neither IgG2c (Fig. 1G) nor IgG2b (not shown). Although tertiary immunization appeared to induce relatively stable levels of RBD-specific IgG in both groups, the NAb titers were still found significantly higher in WT mice compared to TLR7-deficient mice at the two time points tested (Fig. 1H). Spleens were analyzed at the time of sacrifice (d+147) to quantify the numbers of $CD138^+$ plasma cells (PC) and GL7 GC B cells in the spleen (Fig. S3A-C). Both PC numbers and GC B cells were dramatically reduced in TLR7-deficient mice (Fig. S3B,C). Anatomical GC structures in the spleens of BPL-SARS-CoV2 immunized mice were also identified by wide-field imaging in WT mice (Fig. S3D). Such structures were not found in TLR7-deficient mice (Fig. S3E). Together, these data show that TLR7 is required for the optimal development of high titers of NAb upon vaccination with BPL-inactivated SARS-CoV2 associated with GC response. TLR7-deficient mice fail to mount the Myd88-dependent IgG2b and IgG2c isotypes and only produced RBD-specific class-switched IgG1, with no GC development.

Crucial role of TLR7 in augmenting RBD-specific B-cell responses to the PLA vaccine AP205-RBD

The bacterial phage-derived VLPs AP205-RBD mimics SARS-CoV2 virus structurally and contains bacterial ssRNA that can stimulate TLR7 and downstream Myd88-signaling in murine B cells [10, 14, 17]. AP205-RBD has recently been shown to elicit strong RBD-specific NAb against SARS-CoV2 in mice and macaques, and robust immune protection upon challenge with live virus [17]. Because PLAs have been shown to initiate adaptive B-cell immunity through similar mechanisms as inactivated viruses [15], we next sought to determine the contribution of TLR7-signaling in the protective RBD-specific antibody response induced by the AP205-RBD vaccine. WT or TLR7-deficient B6 mice were immunized i.p. with AP205-RBD twice 3 weeks apart as previously shown [17]. Strong RBD-specific antibody responses were detected in WT mice but not in TLR7-deficient mice, which not failed to develop RBD-specific IgG2b and IgG2c, but also IgG1 (Fig. 2A–D). Total serum IgM and IgG concentrations were not significantly different between WT and TLR7-deficient mice, although a trend towards lower levels of IgG was observed (Fig. S4) as previously reported [22]. In accordance with previous studies, the hierarchy of RBD-specific isotypes was IgG2c>IgG2b>IgG1 in AP205-RBD immunized mice (Fig. 2B,C,D) [17]. At day 66 postimmunization we assessed the frequency of RBD-specific B cells using RBD-BV711 and RBD-APC tetramer labeling of splenic B cells (Fig. 2E). The gating strategy is shown in Fig. S5. Whereas the relative frequencies of $CD19^+$ B cells or class-switched IgD^-IgM^- (swIg) B cells were similar between both groups, the proportion of RBD-specific B cells among swIg B cells was significantly reduced in TLR7-deficient mice (Fig. 2F). In agreement with a previous report, AP205-RBD induced a long-lasting antigen-specific GC response, which could be detected 2 months after secondary challenge [17]. Of note, GC B cells were undetectable in TLR7-deficient mice (Fig. 2G). RBD-specific swIg memory B cells were, however, found within the swIg B cell pool in TLR7 KO mice, although at reduced frequency compared to TLR7 sufficient mice (Fig. 2H). Similar results were obtained by measuring the RBD-specific B cells at earlier time points of the immune response (Fig. S6). The proportion of RBD-specific GC B cells (Fig. S6D), as well as $CD38^+$ $GL7^-$ memory B cells (Fig. S6E), were markedly reduced in TLR7-deficient mice by day 11 postimmunization. Together, these data demonstrate the non-redundant role of TLR7-signaling in the antigen-specific GC response to immunization with ssRNA-loaded PLAs AP205-RBD.

T-cell-dependent antibody response to PLA-based COVID-19 vaccine requires B cell-intrinsic TLR7

Because the physical association of the B-cell antigen and the TLR7 ligands is required to elicit RBD-specific Ab responses and GC reaction [17], we then examined whether B-cell-intrinsic TLR7-signaling was necessary to promote RBD-specific antibody responses to AP205-RBD. Rag2-deficient B6 mice were adoptively transferred with WT $CD4^+$ T cells and $CD19^+$ B cells from either WT or TLR7 KO mice prior to immunization with AP205-RBD twice 4 weeks apart. In the absence of $CD4^+$ T-cell transfer, RBD-specific Ab responses were below the GMFI value of 10 for all isotypes (not shown). The production of RBD-specific IgG2b and IgG2c was significantly reduced in the group transferred with TLR7-deficient B cells, whereas IgG1 production was similar between mice transferred with WT or TLR7 KO B cells (Fig. 3A–C). Analysis of splenic B cells revealed significant downregulation of IgD^-IgM^- swIg B cells and RBD-specific memory and $GL7^+$ GC B cells in mice adoptively transferred with TLR7 KO compared with WT B cells (Fig. 3D–G). Likewise, GC structures were identified by immunostaining of spleen cryostat sections in mice adoptively transferred with WT B cells but not with TLR7-deficient B lymphocytes (Fig. 3H–J). Together, these results demonstrate the role of B-cell-intrinsic TLR7 for optimal GC reaction and antibody response against AP205-RBD, providing a mechanistic explanation for the in vivo mode of action of this PLA-based COVID-19 vaccine candidate.

Conclusion

The ssRNA-sensing TLR7 has recently emerged as a critical innate receptor in the initial control of the spreading of SARS-CoV2 through its capacity to promote the early release of type I IFN, most likely by pDCs in the respiratory tract [4, 7, 23]. In the present study, we establish that TLR7 is also critical for the development of a protective RBD-specific humoral immune response to the PLA-based COVID-19 vaccine AP205-RBD or inactivated SARS-CoV2. B-cell-intrinsic TLR signaling has been shown to be essential to initiate CD4 T-cell-dependent antiviral humoral immune responses and GC responses in multiple studies in response to PLAs [10-14, 24, 25]. Here, we now show that the critical dependency of TLR7-driven activation in B-cell-driven immunity also applies to inactivated SARS-CoV2 and the AP205-RBD vaccine. It is likely that similar mechanisms are at play in the induction of protective humoral immunity in response to inactivated viruses or virus-derived nanoparticle antigens [15]. Indeed, it has recently been reported that B-cell-mediated antigen-presentation initiates CD4 T-cell responses to phage Qβ-derived VLPs or inactivated influenza virus, thereby generating GCs [15]. Detailed analysis of the early steps of GC reaction to Qβ-VLP has shown that cell-intrinsic TLR-signaling promotes B-cell proliferation, induction of $Bcl\text{-}6^+$ GC B-cell precursors, and the production of B-cell-derived factors promoting naïve CD4 T-cell differentiation to T_{FH} and Th1 cells [14, 15]. Thus, as reported for other PLAs cells [14, 15, 24, 25], our data indicate that TLR7 signaling in B cells is also essential to promote the output of RBD-specific plasma cells and memory B cells by enhancing the initial GC selection of antigen-specific B in response to AP205-RBD.

The dependency on TLR7 may not apply to other types of vaccines, such as adjuvanted soluble antigens or mRNA vaccines, which are likely to preferentially target DCs [17]. A recent

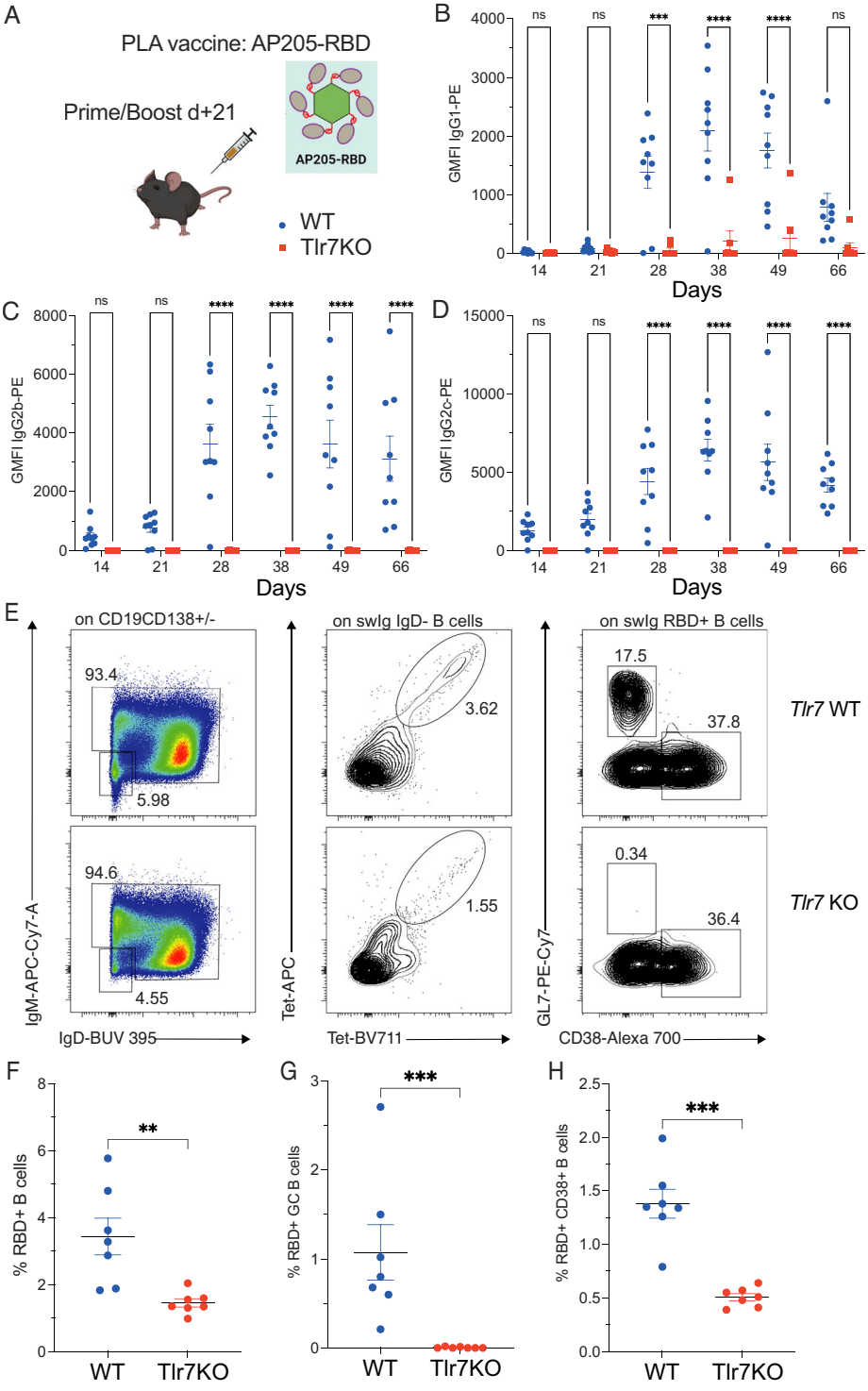

Figure 2. TLR7 is required for RBD-specific IgG antibody production and GC reactions in response to the PLA-based COVID-19 vaccine AP205-RBD. (A) Experimental design of the experiment. WT and TLR7-deficient B6 female mice were immunized i.p. with AP205-RBD (3 μg/mouse) and challenged with the same dose at day 21. The relative production of RBD-specific IgG isotypes IgG1 (B), IgG2b (C), and IgG2c (D) was quantified in mouse sera at the indicated time points using the HAT-Flow assay. Results are expressed as GMFI from individual mice (mean ± SEM). Statistical differences between groups were analyzed using a two-way-ANOVA followed by Sidak's multiple comparison test. (E–H) At day 66 post-immunization, spleen cells were assessed for RBD-specific B cells as shown in Fig. S5. (E) $CD19^+$ IgM^-IgD^- swIg B cells were assessed for the expression of RBD-specific B cells ($RBD\text{-}APC^+/RBD\text{-}BV711^+$), and the relative proportion of GC B cells ($GL7^+CD38^-$) and memory B cells ($GL7^-CD38^+$). Summary data are shown in (F-H), frequencies of RBD^+ (F), RBD^+ $GL7^+$ (G), or RBD^+ memory (H) B cells among swIg B cells. Results are representative of two experiments performed. Statistical differences were analyzed using a Mann-Whitney test. **, $p < 0.01$; ***, $p < 0.001$; ****, $p < 0.0001$.

study investigating the humoral responses against SARS-CoV2 in mRNA-vaccinated individuals with a deficiency in TLR7, IRF7, or IFNAR1, showed that the RBD-specific IgG responses were largely unaffected up to 7 months after vaccination [26]. However, only one single TLR7 loss-of-function subject was tested in this study, the results suggested that TLR7 could be dispensable for mRNA vaccine-driven humoral responses. In contrast, results obtained in Myd88-deficient mice showed that Tfh and GC B-cell responses were greatly diminished upon immunization with lipid-nanoparticle-based mRNA vaccines [27]. Whether B-cell TLR7 signaling plays a role in this setting will deserve further investigation.

TLR7 is encoded on the X chromosome and escapes X chromosome inactivation in subsets of immune cells, including B cells

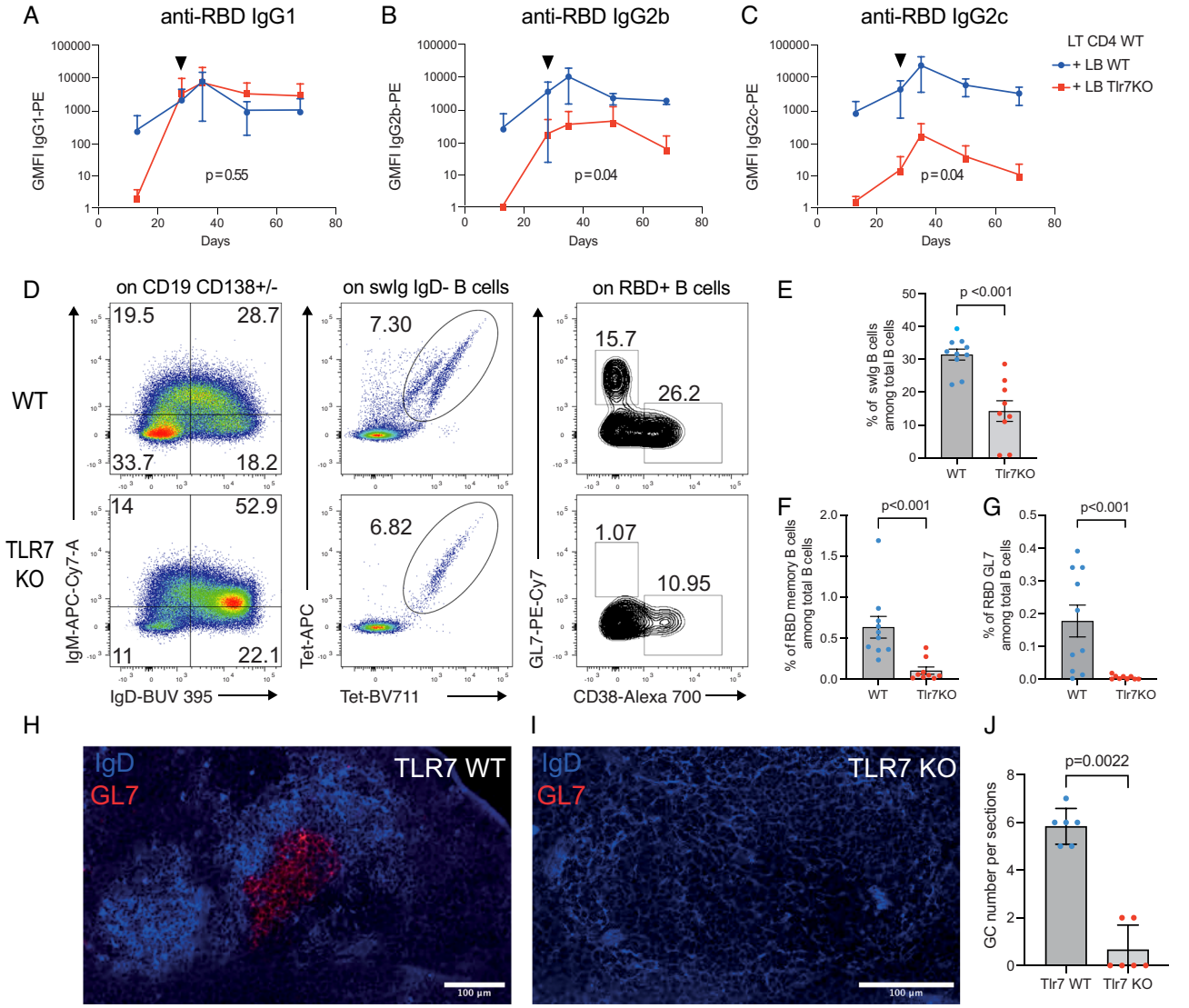

Figure 3. B-cell-intrinsic TLR7 is required for Ig class-switch recombination to RBD-specific IgG2b/IgG2c and the GC response to AP205-RBD immunization. Rag2-deficient B6 mice were injected i.v. with purified naive CD4$^+$ T cells (5×10^6/mouse) together with purified CD19$^+$ B cells (10^7/mouse) from either WT (n = 3) or TLR7-deficient (n = 4) B6 mice prior immunization with AP205-RBD twice at 4 weeks interval. (A–C) The kinetics of RBD-specific IgG1 (A), IgG2b (B), and IgG2c (C) activity was measured in serum. Two way-ANOVA was used to assess statistical differences between curves. Results shown are representative of two experiments. At days 15 to 38 postsecondary challenge, the RBD-specific B cells were assessed in the spleen as shown in Fig. S5. (D) CD19$^+$ IgM$^-$IgD$^-$ swIg B cells were assessed for the expression of RBD-specific B cells (RBD-APC$^+$/RBD-BV711$^+$), and the relative proportion of GC B cells (GL7$^+$CD38$^-$) and memory B cells (GL7$^-$CD38$^+$). Summary data are shown in (E–G), frequency of swIg B cells (E), RBD$^+$ memory (F), or GL7$^+$ (G) B cells among total B cells. Results were pooled from three independent experiments. Results from individual mice (9–10 mice/group) are shown with mean ± SEM. Spleen cryostat sections from Rag2$^{-/-}$ mice adoptively transferred with either WT (H) or TLR7 KO (I) B lymphocytes were stained for GC structure with anti-IgD (blue) and anti-GL7 (red) antibodies and acquired using a wide-field microscope. (J) The numbers of GC structures were counted from three cryostat sections per spleen and data from individual mice are shown with mean ± SD. Statistical differences between groups were analyzed using a Mann–Whitney test.

[28]. This is associated with enhanced TLR7 protein expression in women compared to men, and superior functional responses of B cells with biallelic expression of TLR7 [28]. Of note, anti-Spike antibodies and RBD-specific NAbs declined faster in males than in females, independently of age, suggesting an association of sex with the evolution of the humoral response during the course of natural COVID-19 [29, 30]. Recently, female mice have been reported to generate more robust antibody responses to Influenza A virus (IAV) vaccines in comparison to males, associated with enhanced GC responses and affinity maturation [25, 31]. This sex bias was lost in TLR7-deficient mice, suggesting that greater TLR7 activation in females may improve the efficacy of IAV vaccination [25]. Whether PLA-based vaccines may promote accelerated GC reactions and enhanced protective antibody responses in females through a genetic effect of the X chromosome warrants further investigation.

Materials and methods

Mice

Female mice 8 to 12-week-old C57BL/6J (B6), Rag2-deficient B6 (B6.Cg-Rag2/J) or B6.129S1- *Tlr7*^{tm1Flv}/J were used in the present study. B6.129S1- *Tlr7*^{tm1Flv}/J and B6.Cg-Rag2/J mice were purchased from the Jackson Laboratory and were subsequently bred and housed in our animal facility (INSERM UMS06, Toulouse, France). Animals were housed in specific pathogen-free conditions. All mice were handled according to the Animal Care and Use of Laboratory guidelines of the French Ministry of Research (APAFIS#15236-2018052212322298).

Virus preparation and inactivation

SARS-CoV2 (Occitanie/2020/sCoV2-006) was grown on Vero E6 cells (ATCC) in DMEM (Dutscher) supplemented with 100 U/mL penicillin, 100 μg/mL streptomycin (Invitrogen), and 2% heat-inactivated fetal bovine serum (FBS) (Sigma). Viral stocks were propagated in 300 cm^2 flasks (Dutscher) on which 10^3 tissue culture infectious dose 50 ($TCID_{50}$) of the virus were inoculated in 100 mL infection media for 3 days at 37°C with 5% CO_2. Virus (culture supernatant) was harvested and inactivated with BPL (Fischer) overnight at 4°C. The virus was concentrated by ultracentrifugation, resuspended in PBS, and stored at −80°C until use as described [9].

SARS-CoV2 seroneutralization assay

Serial dilutions of mouse sera were tested in triplicate for their capacity to neutralize the infectivity of native SARS-CoV2 viruses (Occitanie/2020/sCoV2-006) to infect Vero E6 cells cultured as above. Prediluted sera were mixed at 1:1 ratio with diluted virus (100 $TCID_{50}$ per well) and incubated 1 h at 37°C before addition to 96-well plates pre-cultured with Vero E6 cells. The virus/sera mixture was incubated on Vero E6 cells for 2 h at 37°C and then removed, before the addition of 200 μL complete DMEM medium. Cultures were incubated at 37°C and cytopathogenic effect read day 3 postinfection. Antibody titers were expressed as the reciprocal of the highest serum dilution that showed absence of cytopathogenic effect.

Flow cytometry-based assay for RBD-specific IgG isotype quantification

The protocol was adjusted from the one detailed in Townsend et al., [18]. In brief, human O^- red blood cells (RBC, 10×10^6/100 μL) were incubated in a 96 well-plate for 30 min at room temperature with IH4-RBD (2 μg/mL) or IH4 alone (1 μg/mL) as a control. RBC were washed twice with MACS buffer (PBS with 1% FBS, 2mM EDTA) and incubated with pre-diluted sera to be tested (1/200 final dilution in MACS buffer) for 30 minutes at room temperature. RBC were washed twice in MACS buffer and divided into three replicates for isotype determination. Each replicate was incubated for 30 min at room temperature with biotinylated isotype-specific monoclonal antibody: either IgG1 (BD Pharmingen clone A85-1), IgG2b (BD Pharmingen clone R12-3), or IgG2ab (BD Pharmingen clone 5.7). Cells were washed with MACS buffer. RBC were then incubated for 20 min at room temperature and in the dark with Streptavidin-PE (eBioscience). Cells were washed in MACS buffer. RBC were then resuspended in MACS buffer and analyzed for PE-staining by flow cytometry with MACSQuant10 (Miltenyi Biotec) or LSR Fortessa (BD Biosciences). GMFI were obtained by analysis with the FlowJo software V10.

Flow cytometry

Splenocytes were incubated with Fixable Viability Dye eFluor™ 506 (Invitrogen) for 5 min at 4°C. Cells were stained for the specificity of AP205-RBD for 1h on ice with fluorescently labeled RBD tetramer (Miltenyi Biotec), prepared separately beforehand following manufacturer's instructions using streptavidin-PE, -APC (eBioscience) or BV711 (Biolegend). Then, single-cell suspensions were blocked with MACS buffer, containing 2% rat serum and 5 μg/mL anti-CD16/CD32 (2.4G2) and stained for 30 min on ice with the following fluorophore-conjugated antibodies: CD19-BV785 (BD Horizon, clone 1D3), CD138-BV605 (BD Horizon, clone 281–2), IgM-APC-Cy7 (Invitrogen, clone II/41), IgD-BUV395 (BD Horizon, clone 11–26c.2a), GL7-PE-Cy7 (Biolegend, clone GL7), and CD38-AF700 (Invitrogen, clone 90). Cells were analyzed by flow cytometry with a Fortessa X20 (BD Biosciences). Flow cytometry analyses were performed with FlowJo software V10, following the guidelines for the use of flow cytometry in immunological studies [32].

Wide-field imaging of GC structures

Spleens were harvested and embedded in cryo medium OCT (Cellpath). Spleen sections were cut at 8-μm thickness on a cryostat microtome (CM 1950, Leica), thaw-mounted onto superfrost slides (Thermo Scientific), and fixed in acetone. After rehydration in PBS with 5% BSA, the sections were stained with GL7-PE (BD, clone GL7) and IgD-BV421 (Biolegend, clone 11–26c) for 3 h. The slides were then washed in PBS and mounted using Vectashield mounting medium (Vector Labs) before analysis on a wide-field microscope (Zeiss, Axiovert A1).

Data analysis and statistics

FACS analyses were performed using FlowJo software v10 (TreeStar). Statistical analyses were carried out using the Prism v10 software (GraphPad).

Acknowledgements: We are indebted to the core facilities at INFINITY INSERM U1291 and INSERM US006. We are grateful to Alain Townsend for providing the IH4-RBD reagent. This work was supported by grants from Agence Nationale de la Recherche (ANR-20-COV8-0004-01 and ANR-20-CE15-0014-01).

Conflict of interest: The authors declare no commercial or financial conflict of interest.

Author contributions: C.H.M., B.H., and J.C.G. conceived and designed the study. C.H.M., F.A., C.F.L., M.D., and C.C. performed experiments and analyzed the data. M.D. and J.C.G. analyzed the data. B.H. and E.J. contributed essential reagents. J.C.G. wrote the manuscript with input from the co-authors. All authors read and approved the final version of the manuscript.

Data availability statement: The data that support the findings of this study are presented in this paper. No shared databases were used or created.

Peer review: The peer review history for this article is available at https://publons.com/publon/10.1002/eji.202350437

References

1 **Reizis, B.**, Plasmacytoid dendritic cells: development, regulation, and function. *Immunity* 2019. **50**: 37–50.

2 **Hua, Z. and Hou, B.**, The role of B cell antigen presentation in the initiation of CD4+ T cell response. *Immunol. Rev.* 2020. **296**: 24–35.

3 **Barreiro, L. B., Ben-Ali, M., Quach, H., Laval, G., Patin, E., Pickrell, J. K., Bouchier, C. et al.**, Evolutionary dynamics of human Toll-like receptors and their different contributions to host defense. *PLos Genet.* 2009. **5**: e1000562.

4 **Made van der, C. I., Simons, A., Schuurs-Hoeijmakers, J., Heuvel van den, G., Mantere, T., Kersten, S., Deuren van, R. C. et al.**, Presence of genetic variants among young men with severe covid-19. *JAMA* 2020. **324**: 663–673.

5 **Fallerini, C., Daga, S., Mantovani, S., Benetti, E., Picchiotti, N., Francisci, D., Paciosi, F. et al.**, Association of Toll-like receptor 7 variants with life-threatening COVID-19 disease in males: findings from a nested case-control study. *Elife* 2021. **10**.

6 **Solanich, X., Vargas-Parra, G., Made van der, C. I., Simons, A., Schuurs-Hoeijmakers, J., Antoli, A., Del Valle, J. et al.**, Genetic screening for TLR7 variants in young and previously healthy men with severe covid-19. *Front. Immunol.* 2021. **12**: 719115.

7 **Asano, T., Boisson, B., Onodi, F., Matuozzo, D., Moncada-Velez, M., Maglorius Renkilaraj, M. R. L., Zhang, P. et al.**, X-linked recessive TLR7 deficiency in ~1% of men under 60 years old with life-threatening COVID-19. *Sci. Immunol* 2021. **6**: eabl4348.

8 **Onodi, F., Bonnet-Madin, L., Meertens, L., Karpf, L., Poirot, J., Zhang, S. Y., Picard, C. et al.**, SARS-CoV-2 induces human plasmacytoid predendritic cell diversification via UNC93B and IRAK4. *J. Exp. Med.* 2021. **218**: e20201387.

9 **Cenac, C., Ducatez, M. F. and Guery, J. C.**, Hydroxychloroquine inhibits proteolytic processing of endogenous TLR7 protein in human primary plasmacytoid dendritic cells. *Eur. J. Immunol.* 2022. **52**: 54–61.

10 **Hou, B., Saudan, P., Ott, G., Wheeler, M. L., Ji, M., Kuzmich, L., Lee, L. M. et al.**, Selective utilization of Toll-like receptor and MyD88 signaling in B cells for enhancement of the antiviral germinal center response. *Immunity* 2011. **34**: 375–384.

11 **Browne, E. P.**, Toll-like receptor 7 controls the anti-retroviral germinal center response. *PLoS Pathogens* 2011. **7**: e1002293.

12 **Walsh, K. B., Teijaro, J. R., Zuniga, E. I., Welch, M. J., Fremgen, D. M., Blackburn, S. D., von Tiehl, K. F. et al.**, Toll-like receptor 7 is required for effective adaptive immune responses that prevent persistent virus infection. *Cell Host Microbe.* 2012. **11**: 643–653.

13 **Clingan, J. M. and Matloubian, M.**, B Cell-intrinsic TLR7 signaling is required for optimal B cell responses during chronic viral infection. *J. Immunol.* 2013. **191**: 810–818.

14 **Tian, M., Hua, Z., Hong, S., Zhang, Z., Liu, C., Lin, L., Chen, J. et al.**, B cell-intrinsic MyD88 signaling promotes initial cell proliferation and differentiation to enhance the germinal center response to a virus-like particle. *J. Immunol.* 2018. **200**: 937–948.

15 **Hong, S., Zhang, Z., Liu, H., Tian, M., Zhu, X., Zhang, Z., Wang, W. et al.**, B cells are the dominant antigen-presenting cells that activate naive CD4(+) t cells upon immunization with a virus-derived nanoparticle antigen. *Immunity* 2018. **49**: 695–708 e694.

16 **Mohsen, M. O., Zha, L., Cabral-Miranda, G. and Bachmann, M. F.**, Major findings and recent advances in virus-like particle (VLP)-based vaccines. *Semin. Immunol.* 2017. **34**: 123–132.

17 **Guo, C., Peng, Y., Lin, L., Pan, X., Fang, M., Zhao, Y., Bao, K. et al.**, A pathogen-like antigen-based vaccine confers immune protection against SARS-CoV-2 in non-human primates. *Cell Rep. Med.* 2021. **2**: 100448.

18 **Townsend, A., Rijal, P., Xiao, J., Tan, T. K., Huang, K. A., Schimanski, L., Huo, J. et al.**, A haemagglutination test for rapid detection of antibodies to SARS-CoV-2. *Nat. Commun.* 2021. **12**: 1951.

19 **Grzelak, L., Temmam, S., Planchais, C., Demeret, C., Tondeur, L., Huon, C., Guivel-Benhassine, F. et al.**, A comparison of four serological assays for detecting anti-SARS-CoV-2 antibodies in human serum samples from different populations. *Sci. Transl. Med.* 2020. **12**.

20 **Horndler, L., Delgado, P., Abia, D., Balabanov, I., Martinez-Fleta, P., Cornish, G., Llamas, M. A. et al.**, Flow cytometry multiplexed method for the detection of neutralizing human antibodies to the native SARS-CoV-2 spike protein. *EMBO Mol. Med.* 2021. **13**: e13549.

21 **Pinero, P., Marco De La Calle, F. M., Horndler, L., Alarcon, B., Uribe Barrientos, M., Sarmiento, H. and Tarin, F.**, Flow cytometry detection of sustained humoral immune response (IgG + IgA) against native spike glycoprotein in asymptomatic/mild SARS-CoV-2 infection. *Sci. Rep.* 2021. **11**: 10716.

22 **Soni, C., Wong, E. B., Domeier, P. P., Khan, T. N., Satoh, T., Akira, S. and Rahman, Z. S.**, B cell-intrinsic TLR7 signaling is essential for the development of spontaneous germinal centers. *J. Immunol.* 2014. **193**: 4400–4414.

23 **Zhang, Q., Bastard, P., Effort, C. H. G., Cobat, A. and Casanova, J. L.**, Human genetic and immunological determinants of critical COVID-19 pneumonia. *Nature* 2022. **603**: 587–598.

24 **Krueger, C. C., Thoms, F., Keller, E., Leoratti, F. M. S., Vogel, M. and Bachmann, M. F.**, RNA and toll-like receptor 7 license the generation of superior secondary plasma cells at multiple levels in a B cell intrinsic fashion. *Front. Immunol.* 2019. **10**: 736.

25 **Fink, A. L., Engle, K., Ursin, R. L., Tang, W. Y. and Klein, S. L.**, Biological sex affects vaccine efficacy and protection against influenza in mice. *Proc. Natl. Acad. Sci. U. S. A.* 2018. **115**: 12477–12482.

26 **Sokal, A., Bastard, P., Chappert, P., Barba-Spaeth, G., Fourati, S., Vanderberghe, A., Lagouge-Roussey, P. et al.**, Human type I IFN deficiency does not impair B cell response to SARS-CoV-2 mRNA vaccination. *J. Exp. Med.* 2023. **220**.

27 **Alameh, M. G., Tombacz, I., Bettini, E., Lederer, K., Sittplangkoon, C., Wilmore, J. R., Gaudette, B. T. et al.**, Lipid nanoparticles enhance the efficacy of mRNA and protein subunit vaccines by inducing robust T follicular helper cell and humoral responses. *Immunity* 2021. **54**: 2877–2892 e2877.

28 **Souyris, M., Cenac, C., Azar, P., Daviaud, D., Canivet, A., Grunenwald, S., Pienkowski, C. et al.**, TLR7 escapes X chromosome inactivation in immune cells. *Sci Immunol* 2018. **3**: eaap8855.

29 **Grzelak, L., Velay, A., Madec, Y., Gallais, F., Staropoli, I., Schmidt-Mutter, C., Wendling, M. J. et al.**, Sex differences in the evolution of neutralizing antibodies to SARS-CoV-2. *J. Infect. Dis.* 2021. **224**.

30 **Gallais, F., Gantner, P., Bruel, T., Velay, A., Planas, D., Wendling, M. J., Bayer, S. et al.**, Evolution of antibody responses up to 13 months after SARS-CoV-2 infection and risk of reinfection. *EBioMedicine* 2021. **71**: 103561.

31 **Ursin, R. L., Dhakal, S., Liu, H., Jayaraman, S., Park, H. S., Powell, H. R., Sherer, M. L. et al.**, Greater breadth of vaccine-induced immunity in females than males is mediated by increased antibody diversity in germinal center B cells. *mBio* 2022. **13**: e0183922.

32 **Cossarizza, A., Chang, H. D., Radbruch, A., Akdis, M., Andra, I., Annunziato, F., Bacher, P. et al.**, Guidelines for the use of flow cytometry and cell sorting in immunological studies. *Eur. J. Immunol.* 2017. **47**: 1584–1797.

Abbreviations: **BPL**: beta-propiolactone · **GC**: germinal center · **pDCs**: plasmacytoid dendritic cells · **PLA**: pathogen-like antigen · **RBD**: receptor binding domain · **TLR7**: toll-like receptor 7 · **VLP**: virus-like particles

Full correspondence: Dr. Jean-Charles Guéry, PhD, Institut Toulousain des Maladies Infectieuses et Inflammatoires (INFINITY), INSERM UMR1291, Centre Hospitalier Universitaire Purpan, Place du Dr Baylac, 31024 Toulouse Cedex 3, France
e-mail: jean-charles.guery@inserm.fr

Received: 15/2/2023
Revised: 16/5/2023
Accepted: 13/6/2023